



# Osteological and vascular morphology and electrolyte homeostasis of sea turtles

Masataka YOSHIDA<sup>1,2)\*</sup>, Masaharu MOTOKAWA<sup>3)</sup> and Hideki ENDO<sup>1)</sup>

<sup>1)</sup>The University Museum, The University of Tokyo, Tokyo, Japan

<sup>2)</sup>Department of Biological Sciences, Graduate School of Sciences, The University of Tokyo, Tokyo, Japan

<sup>3)</sup>The Kyoto University Museum, Kyoto University, Kyoto, Japan

**ABSTRACT.** Sea turtles have well developed lacrimal glands for their electrolyte homeostasis. In turtles, stapedia artery and palatine artery send branches to supply orbital region, but supply artery for lacrimal glands was not identified. Micro-CT scans showed dorsoventrally large lacrimal glands of sea turtle are supplied by both stapedia artery and palatine artery. The circulatory pattern in cranial region was reconstructed based on the micro-CT scans, showing that sea turtle has basically similar pattern with the common snapping turtle: stapedia artery supplies orbital region and mandibular artery is ramified from stapedia artery. We also investigate the *foramen stapedia-temporalis* in turtles using osteological specimens. The *foramen stapedia-temporalis*, where the stapedia artery passes through, has different size among four families of turtles. We compared the sum of cross sections of left and right *foramen stapedia-temporalis* since homeostasis of one individual is maintained by a pair of lacrimal glands. The size difference may reflect primarily the share of stapedia artery against palatine artery in cranial circulation pattern and blood supply of orbital regions. Our observations confirmed a significantly larger cross-section in the *foramen stapedia-temporalis* of sea turtles than other freshwater/terrestrial turtles. Since the circulatory pattern is shared, the size difference of *foramen stapedia-temporalis* reflects the amount of arterial blood supply to lacrimal glands. Therefore, the size of the *foramen stapedia-temporalis* may indicate marine adaptation of turtles and are applicable to both fossil and osteological specimens.

**KEYWORDS:** Cheloniidae, lacrimal gland, marine adaptation, osteology, stapedia artery

*J. Vet. Med. Sci.*

84(7): 1001–1009, 2022

doi: 10.1292/jvms.21-0624

Received: 22 November 2021

Accepted: 20 May 2022

Advanced Epub:

2 June 2022

Sea turtles (order Testudines, superfamily Chelonioidea) depend on the salt glands in their orbital region for electrolyte homeostasis [23, 45]. Eliminating seawater salts is essential to maintaining electrolyte homeostasis and avoiding dehydration [18, 45]. Sea turtles use salt glands to eliminate excessive salts. The homeostatic burden is reflected in an increase or a decrease in fluid secretion from the salt glands [31, 37, 42, 43]. Lesion or disorder in salt glands result failure to maintain electrolyte homeostasis and may cause death of sea turtles [39]. Other marine or estuarine reptiles and birds also use salt excretion glands in the cranial regions [45]. This may be because, unlike mammals, reptiles and birds do not have efficient kidneys, which produce hypersthenuria [45]. Enlarged orbital glands of sea turtles are not yet fully understood, recent studies even suggest the relationship between magnetic sensing and orbital glands [35, 36].

Studies of cranial structure of turtles always face difficulty since observation of structure of interest demands somewhat destructive process including disarticulation [26]. Salt glands are also not directly observable because the organ is encased in the osteological elements of the orbital rim [12]. This positioning of salt glands makes it difficult to measure them without removing the surrounding tissue or bony elements. Carcasses usually begin decomposing from soft tissues at the distal end in sample collection, including the snout and orbit. As a result, there are few sea turtle specimens without decomposed soft tissues. Therefore, using osteological specimens is beneficial to observe relationships between morphological characters and their habitat.

Histological and histochemical studies have revealed turtle have two orbital glands, but there is disagreement over the identity of these glands [41]. One gland is found anterior to the eyeball in the orbit, called harderian gland [1, 12–15, 17, 48] and anterior lacrimal gland [5, 6]. Another gland is found posterior to the eyeball in the orbit, called lacrimal gland [1, 12–15, 17, 48] and harderian gland [5, 6]. Even though the nomenclature is in confusion, it is agreed that posterior gland secretes salts for osmoregulation [5, 15, 16]. In the current study, we follow [16, 48] and use harderian gland for the anterior orbital gland and lacrimal gland for the posterior gland (Fig. 1).

\*Correspondence to: Yoshida, M.: mstkyoshida@um.u-tokyo.ac.jp, Laboratory of Dead Body Science, The University Museum, The University of Tokyo, Hongo 7-3-1, Bunkyo, Tokyo 113-0033, Japan

©2022 The Japanese Society of Veterinary Science



This is an open-access article distributed under the terms of the Creative Commons Attribution Non-Commercial No Derivatives (by-nc-nd) License. (CC-BY-NC-ND 4.0: <https://creativecommons.org/licenses/by-nc-nd/4.0/>)

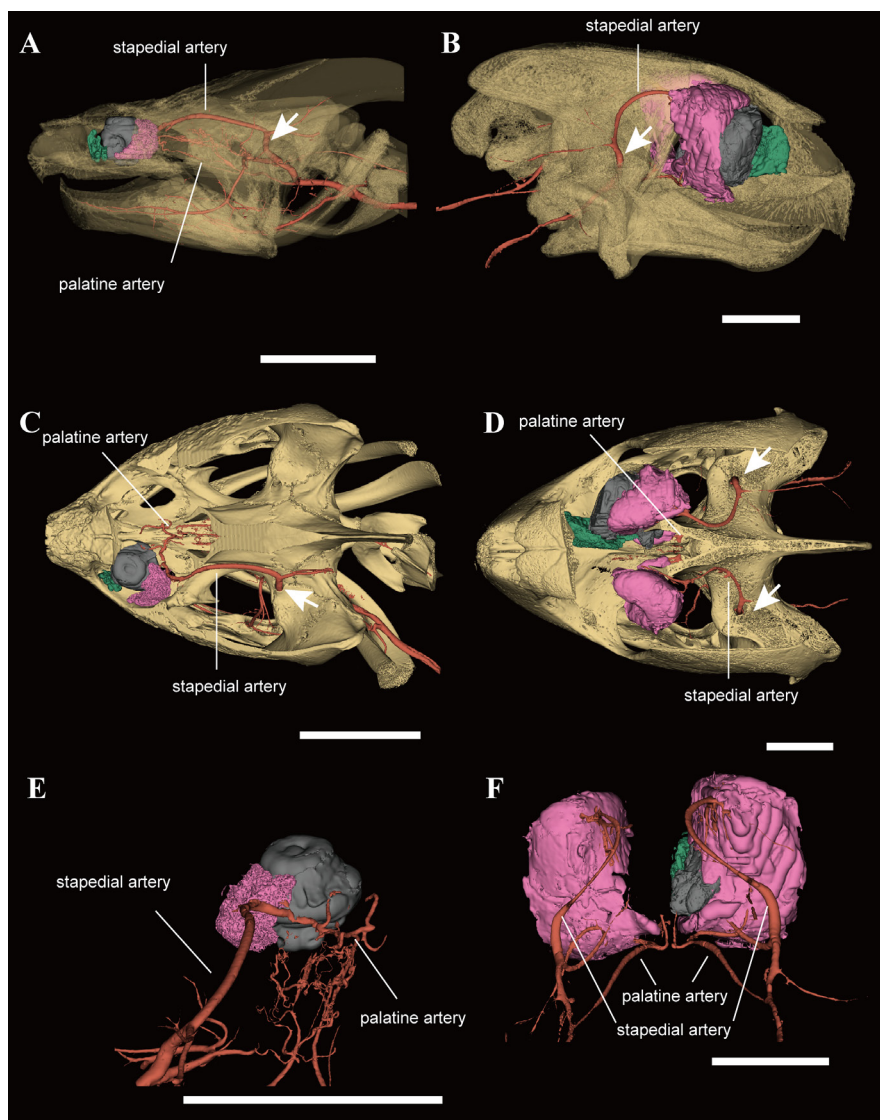


**Fig. 1.** 3D reconstruction of turtle skull. Eyeball is in gray, harderian glands is in green and lacrimal gland is in pink. White arrow indicates position of *foramen*. Each scale bar is 25 mm. **A.** Left lateral view of skull of *Chelydra serpentina*. **B.** Right lateral view of the skull of *Lepidochelys olivacea*. **C.** Dorsal view of skull of *Chelydra serpentina*. Skull roof is removed. **D.** Dorsal view of skull of *Lepidochelys olivacea*. Skull roof is removed. **E.** Posterior view of left eyeball and orbital glands of *Chelydra serpentina*. **F.** Posterior view of right eyeball and both orbital glands of *Lepidochelys olivacea*. Note well-developed stapedial artery supply orbital region in both *Chelydra serpentina* and *Lepidochelys olivacea*.

Orbital region receives arterial blood from the cranial and carotid arteries [1, 3, 25, 27]. The relationships between cranio-vascular morphology and phylogeny in turtles have been discussed [20, 25–27, 44]. Patterns of carotid circulation of turtles and relationship to phylogeny is under discussion [25, 44], but variation between clades have long gathered interests [3, 20, 21, 25–27, 34]. The two arteries, stapedial artery and palatine artery are known to run into orbital region [3, 26]. In sea turtles, the carotid circulation is considered as mostly like other Trionychia turtles in earlier studies [3, 25]. This has been understood as an example of parallel evolution [20, 25] since sea turtles and soft-shelled turtles are not closely related [28]. Internal carotid artery branches stapedial artery posterior to skull. The stapedial artery passes through the *foramen stapedio-temporalis* (FST) from ventral to dorsal and its development is considered as basal character for turtles [3, 21, 25–27, 44]. *Foramen stapedio-temporalis* opens on the dorsal surface of the skull, contributed by protic and quadrate with no flexibility of articulation (Fig. 1).

Arterial wall can adapt by vasodilation for shear stress due to the increase of blood pressure. Artery can remodel and maintain its structure in response to the blood flow and pressure [32]. According to the Poiseuille law, arterial blood flow amount should be related to the diameter of artery and pressure. Arterial circulation primarily vasodilates to increase blood flow before gaining pressure. Reptilian lacrimal gland cells are not capable of excreting salts since water will be lost under hypertension [22]. Also, the stapedial artery send branches for the eyeball and its surrounding capillaries. Rise of blood pressure in these branches affect

intraocular pressure rise and may harm ocular and systemic condition of sea turtles [11]. Thus, when a larger volume of arterial blood should be supplied to salt gland with limited rise of blood pressure, the stapedia arteries for lacrimal glands should vasodilate as much as possible. The vasodilation of stapedia artery is dominated by the *canalis stapedio-temporalis* and FST.

Several lineages of turtles have tried to expand their habitat into ocean and extant superfamily Chelonioidae is one and only successful group among them. At the same time, other lineages of turtles radiate diversified environment. Our study tries to establish the relationship between development of lacrimal glands and ecology, by cranial morphology.

## MATERIALS AND METHODS

We examined 3 fixed specimens and 168 turtle osteological specimens from museum collections. We accessed Kanagawa Prefectural Museum of Natural History, Odawara, Kanagawa, Japan (KPMNH), Kyoto University Museum, Kyoto, Kyoto, Japan (KUZ), National Museum of Nature and Science, Tsukuba, Ibaraki, Japan (NMNS) and The University of Tokyo, Bunkyo, Tokyo, Japan (UMUT).

We obtained micro X-ray computer-tomography scan from head samples of a common Snapping Turtle *Chelydra serpentina* (*Cs*) (UMUT-21293), a hawksbill sea turtle *Eretmochelys imbricata* (*Ei*) (KPM-NFR-526) and a ridley sea turtle *Lepidochelys olivacea* (*Lo*) (NSM-H6187). We used micro X-ray computer-tomography system (TXS-UF225CT; TESCO Corp., Yokohama, Japan) at UMUT. To highlight arteries, we preliminary injected physiological saline solution by physiological pressure into the common carotid artery. Samples are fixed by 80% ethanol after injection. Scans are conducted at 150 kV and 0.15 mA, then reconstructed using 3D Slicer v4.13.0 (<https://www.slicer.org/>) [19]. The intravascular lumen of interested arteries could be distinguished from other soft tissue by the difference of intensity in the 3D reconstructed images (Figs. 1 and 2). Observed intravascular lumen of arteries should be vasodilated by the injected saline solution, with physiological pressure unique to each sample. Therefore, the quantitative comparison of cross section between arteries are possible but inadequate in between samples. At the same time, our observation by micro X-ray computer-tomography scan do not obtain all of circulatory system in cranial region. The 3D reconstruction of *Lo* specimen (NSM-H6187) excludes left eyeball and surrounding tissue for another dissection.

We also obtained cranial sizes for 36 distances [21] using digital calipers on osteological specimens. Measurements were taken from specimens of family Chelydridae (n=23), Cheloniidae (n=99), Kinosternidae (n=1), Emydidae (n=33), Geoemydidae (n=1), Testudinidae (n=10), and Podocnemididae (n=1) (Table 1).

Family Chelydridae specimens included one Alligator Snapping Turtle *Macrochelys temminckii* (*Mt*), and *Cs*. Family Emydidae samples in this research were all Red-eared Slider *Trachemys scripta* (*Ts*). UMUT acquired Snapping Turtle specimens and Red-eared Slider specimens from Chiba Biodiversity Center, Chiba, Japan, from their extermination program for invasive species. Family Cheloniidae specimens included *Chelonia mydas* (*Cm*) and *Caretta caretta* (*Cc*). The sea turtle specimens stored in the KUZ collection were originally collected in collaboration with the Sea Turtle Association of Japan (non-profit organization in Osaka, Japan), based on stranded or bycatch individuals found on the beach. Although available number of examples from family Kinosternidae, Geoemydidae, Testudinidae and Podocnemididae are insufficient to produce a statistically adequate, we added them for comparison. Since cranial-arterial circulation is different in family Kinosternidae [1, 25, 27], extremely small FST is observed in our *Staurotypus triporcatus* sample (UMUT-21018), and the right FST is completely closed.

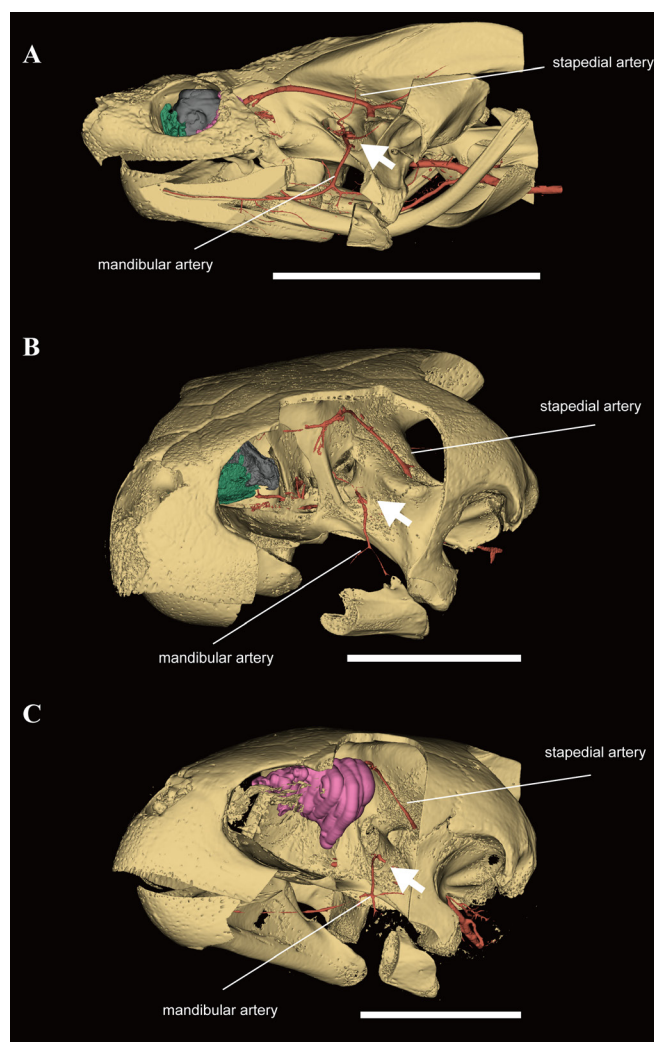


**Fig. 2.** 3D reconstruction of turtle skull, lateral portion removed. Eyeball is in gray, harderian glands is in green and lacrimal gland is in pink. White arrow indicates position of *foramen anteriomandibulare*. Each scale bar is 50 mm. **A.** Left lateral view of *Chelydra serpentina*. **B.** Left lateral view of *Lepidochelys olivacea*. **C.** Left lateral view of *Eretmochelys imbricata*. Mandibular artery of *Lepidochelys olivacea* and *Eretmochelys imbricata* are not vestigial, but distinct as in *Chelydra serpentina*.

**Table 1.** List of examined samples

Family	Genus and specie	Number of samples				Institution
		Total	Male	Female	Unidentified	
Chelydridae	<i>Chelydra serpentina</i>	22	(10)	(12)		UMUT
	<i>Macrochelys temminckii</i>	1		(1)		UMUT
Cheloniidae	<i>Caretta caretta</i>	44	(3)	(22)	(21)	KUZ
		2			(2)	KPMNH
	<i>Chelonia mydas</i>	51	(9)	(26)	(16)	KUZ
		2			(2)	KPMNH
Kinosternidae	<i>Staurotypus triporcatus</i>	1		(1)		UMUT
Emydidae	<i>Trachemys scripta</i>	33	(15)	(18)		UMUT
Geoemydidae	<i>Mauremys japonica</i>	1		(1)		UMUT
Testudinidae	<i>Centrochelys sulcata</i>	1		(1)		UMUT
	<i>Geochelone elegans</i>	3	(1)	(2)		UMUT
	<i>Geochelone platynota</i>	1		(1)		UMUT
	<i>Malacochersus tornieri</i>	1		(1)		UMUT
	<i>Manouria emys</i>	1		(1)		UMUT
	<i>Stigmochelys pardalis</i>	1		(1)		UMUT
	<i>Testudo graeca</i>	1		(1)		UMUT
	<i>Testudo horsfieldii</i>	1		(1)		UMUT
	Podocnemididae	<i>Podocnemys unifilis</i>	1			(1)

KPMNH, Kanagawa Prefectural Museum of Natural History, Odawara, Kanagawa, Japan. KUZ, Zoological Collection of Kyoto University Museum, Kyoto, Kyoto, Japan. UMUT, The University Museum, The University of Tokyo, Bunkyo, Tokyo, Japan.

All the Snapping Turtles, sea turtles, and Red-eared Sliders were from wild environments. Other specimens are came from zoos and aquaria.

The authors obtained body mass and carapace size in the UMUT specimens if the carcasses were not badly damaged. We measured the body size of turtles [24] at straight carapace length (SCL), curved carapace length, straight carapace width, curved carapace width, plastron length and plastron width using calipers and a tape measure. We used the data from the collection catalogue [49] for several turtle specimens stored in the UMUT collection. In those data, body sizes were measured in the same way as in this study.

We obtained the size of the FST indirectly, as direct measurements of osteological foramen using calipers are difficult to achieve [26]. We made casts of each foramen with vinyl polysiloxane impression materials used in dentistry (GC EXAFINE (c) PUTTY; GC Corp., Tokyo, Japan) material). We removed the silicon cast after the solidification by hand. Then, we measured the cast at its maximum (MaD) and minimum (MiD) diameters with a digital micrometer or a digital caliper.  $MaD/2 \times MiD/2 \times \pi$  obtains the cross-sectional area of FST. Then, we added the right and left cross-sectional values to obtain the total FST value for each specimen to represent electrolyte homeostasis capability of individual. In several samples we could only measure one side of the skull and one of two foramina. We doubled the value of one measurable side and regarded it as the FST value. A quantitative comparison of the relative size of cranial foramina between taxa or individuals, requires the effect of body size to be removed. However, all the sea turtle specimens lacked a record of their body mass, and most lacked the body size due to the condition of carcasses in the museum collection. The SCL was recorded for 32 specimens out of 98 specimens. The other 67 specimens lacked any body size records.

The relationships between the skull size and carapace size were calculated [38]. The cranio-caudal length from snout to crista supraoccipitalis is best correlated to SCL. The cranio-caudal length of the skull from the snout to lower jaw articulation is much weakly correlated to SCL. For the 67 specimens without body size data, the estimated size of the SCL was calculated from cranio-caudal length of skull (snout-crista supraoccipitalis). Of these 67 specimens, 66 had complete skull for measuring cranio-caudal length from the snout to the crista supraoccipitalis. One last specimen (KUZR-070202, *Cc*) lacked the crista supraoccipitalis; therefore, we adopted calculations using the cranio-caudal length from snout to lower jaw articulation. Then, we applied another calculation [47] to estimate the body mass of every individual based on the real and estimated carapace size. To illustrate the allometric growth of the FST, we plotted body mass and FST on a scatter chart, log to log scale [33]. Linear regression lines are obtained to indicate the allometric growth of FST of family Chelydridae, family Cheloniidae, family Emydidae and family Testudinidae (Fig. 4). The common logarithm of the cross-sectional area of the FST was divided by the common logarithm of the body mass to obtain the relative value of the size of the FST with body size removed (rFST) (Figs. 5 and 6).

## RESULTS

3D model of arteries and other structure of skull is obtained from the micro-CT scan (Figs. 1 and 2). In *Lo*, in the region of our

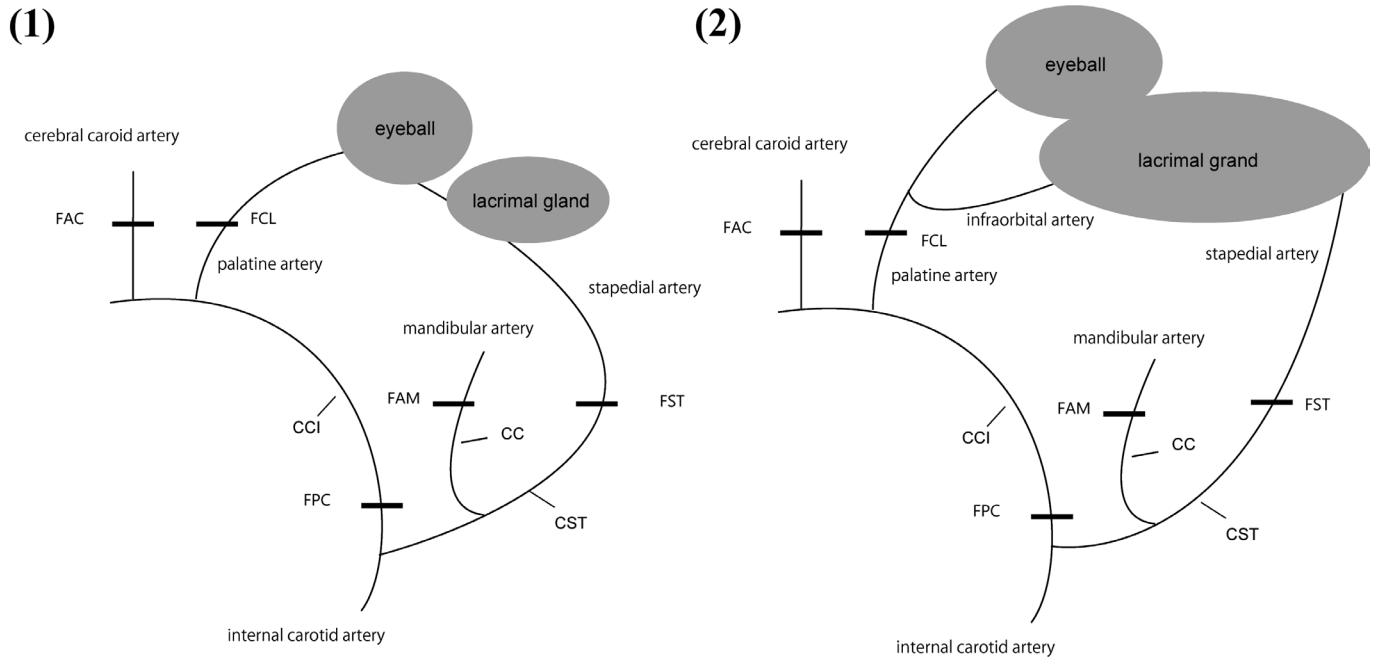


**Fig. 3.** Diagram of right cranial circulation of turtles. In dorsal view, snout toward the top of page. (1) *Chelydra serpentina*. (2) Cheloniidae sea turtle. CCI, *canalis caroticus internus*; CC, *canalis cavernosus*; CST, *canalis stapedio-temporalis*; FAC, *foramen anterior canalis carotici interni*; FAM, *foramen anteriomandibulare*; FCL, *foramen caroticum laterale*; FPC, *foramen posterior canalis carotici interni*; FST, *foramen stapedio-temporalis*.

interest, two arteries supplying orbital glands are confirmed. Palatine arteries give rise to the branch for anterior harderian glands. On the other hand, stapedial artery runs dorsally in fossa temporalis and splits several branches to supply lacrimal glands. Palatine artery also send branch to the ventral part of lacrimal gland and eyeball (Fig. 3(2)).

In *Cs*, palatine artery and stapedial artery bifurcates in the posterior margin of orbital fossa, then send branches to supply lacrimal glands, eyeball, and harder glands (Fig. 3(1)). The size of glands was not obtained since separation of organs were not clear without stain.

The linear regression line of family Chelydridae ( $y=0.3523 \times -0.5572$ ), family Cheloniidae ( $y=0.5362 \times -1.02$ ), family Emydidae ( $y=0.2717 \times -0.5081$ ) and Family Testudinidae ( $y=0.5362 \times -1.02$ ) for allometric growth of FST is obtained (Fig. 4). Allometric growth of FST is hypoallometric in all families, but family Cheloniidae have largest slope suggesting that FST of sea turtles grows faster than others. To determine the comparison between families, we use rFST as FST size with body size removed. rFST of family Chelydridae ( $n=23$ ), family Cheloniidae ( $n=98$ ), family Emydidae ( $n=33$ ), and family Testudinidae ( $n=10$ ) samples are shown in the boxplot (Fig. 5). Family Kinosternidae ( $n=1$ ), family Geoemydidae ( $n=1$ ), and family Podocnemididae ( $n=1$ ) were excluded from the analysis here because there were too few samples available to obtain statistically significant trends. It is notable that Kinosternid turtle *Staurotypus triporcatus* (UMUT-21018) has right FST completely closed. Several *Trachemys scripta* (UMUT-19328 and 19345) have extremely reduced and almost closed FST and their rFST are negative value (Figs. 4–6).

We tested the normality of the distribution of the rFST with the Shapiro–Wilk test. Normality was not rejected for the family Cheloniidae samples ( $P<0.001$ ), but it was for family Chelydridae ( $P=0.6890$ ), family Emydidae ( $P=0.1229$ ), and family Testudinidae ( $P=0.0932$ ). Since the rFST value of family Chelydridae, Emydidae, and Testudinidae were not normally distributed, we used the Kruskal–Wallis test to determine the differences between the four families. rFST values are significantly different between groups ( $P<0.001$ ). Steel–Dwass tests were performed as a post-hoc test to develop multiple comparisons of the four families. Family Cheloniidae was significantly different from family Chelydridae ( $P<0.001$ ), family Emydidae ( $P<0.001$ ), and family Testudinidae ( $P<0.001$ ). Family Chelydridae was also significantly different from family Emydidae ( $P<0.001$ ). Family Testudinidae was not significantly different from family Chelydridae ( $P=0.8595$ ), but it was significantly different from family Emydidae ( $P<0.001$ ).

In family Cheloniidae, *Cc* ( $n=46$ ) was not normally distributed, but *Cm* ( $n=53$ ) was. We performed a Man–Whitney test and found that *Cc* has a significantly larger rFST than *Cm* ( $P<0.001$ ) (Fig. 6). Significantly larger rFST of *Cc* is also observed in comparison of *Cc* female and *Cm* female (Kruskal–Wallis test,  $P=0.0295$ ). Differences by sex occur in *Cm*. In *Chelonia*, males ( $n=9$ ) have significantly smaller rFST than females ( $n=26$ ) (Kruskal–Wallis test,  $P=0.0334$ ) (Fig. 4). Unlike *Chelonia*, the sexual difference is not significant (Kruskal–Wallis test,  $P=0.6587$ ) in *Caretta*. The sampling bias should be taken into account because the specimens of *Cc* had poor records of sexual determination: female ( $n=22$ ), male ( $n=3$ ), and unidentified ( $n=23$ ) (Table 1).

In other families, sexual differences are not found either in *Cs* ( $P=0.3226$ ) or in *Ts* ( $P=0.2328$ ) (Fig. 6).

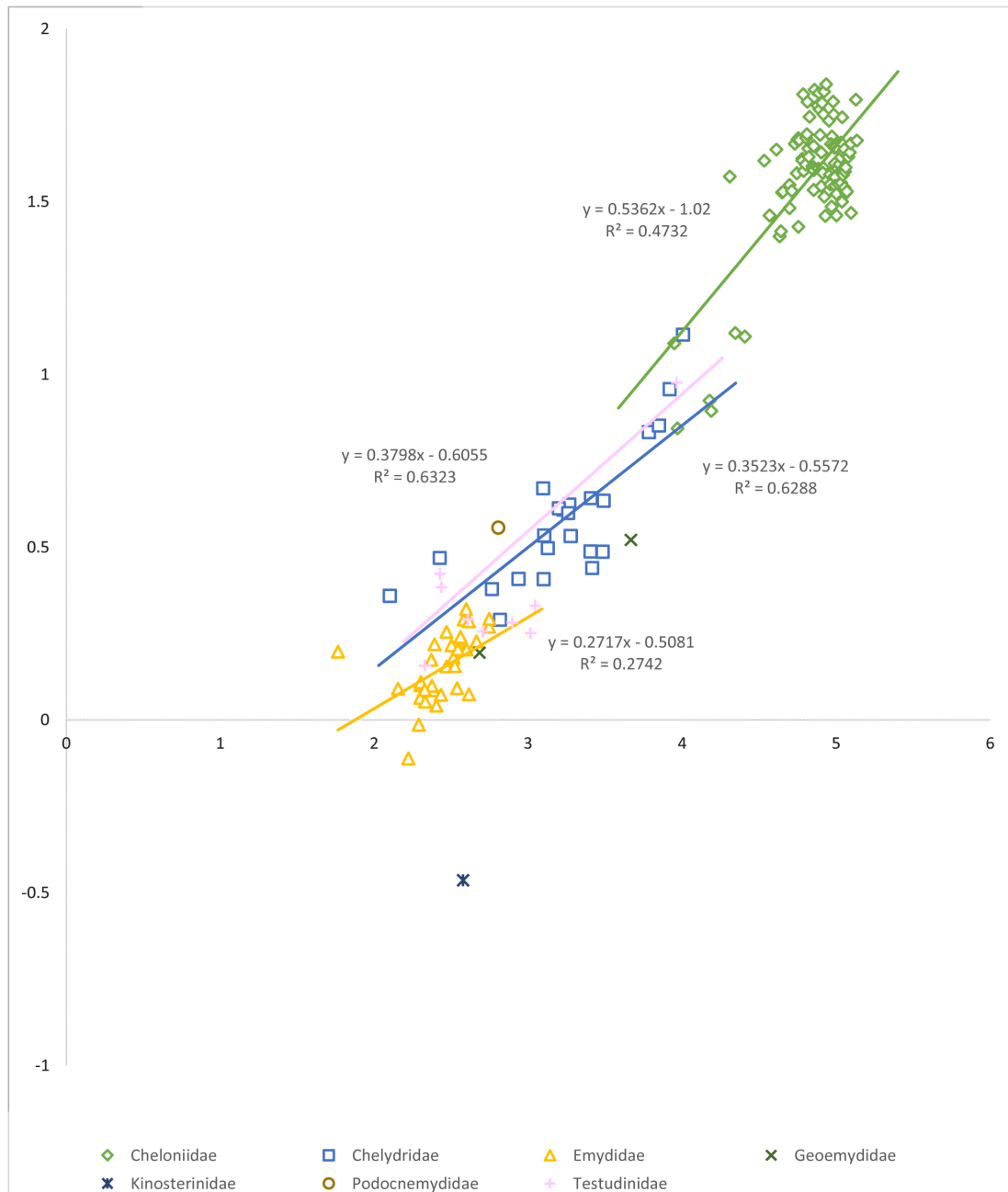


**Fig. 4.** X axis is common logarithm of body mass as the body size and Y axis is the common logarithm of cross section of *foramen stapedio-temporalis*. Body mass includes estimated data calculated from the skull size. Slope shows linear regression of family Chelydridae, family Cheloniidae, family Emydidae and family Testudinidae.

## DISCUSSION

Our reconstruction of circulatory patterns of both *Ei* and *Lo* basically agrees with *Cs*, showing the pattern A [25, 26] (Fig. 3). Our observations on circulatory system of *Ei* and *Lo* (Fig. 3(2)) are different from the observation of *Cm* in previous study [3]. In the observation of *Cm* [3], the cranial region mainly supplied by palatine arteries. In addition, the lower jaw is supplied from the mandibular artery branched from the palatine artery. However, in our observations on *Ei* and *Lo* by micro-CT, the cranial region is mainly supplied by stapedia arteries (Fig. 1B, 1D and 1F, 2B and 2C). The lower jaw region is supplied by the mandibular artery, the branch of stapedia artery (Fig. 2B and 2C). This mandibular artery was considered as “vestigial” in an earlier study [3]. The mandibular artery of *Cs* (Fig. 2A) is also the branch of stapedia artery and agrees with the previous observation [3].

The calculated rFST value for family Cheloniidae is the largest and is significantly different from all other groups. Micro-CT

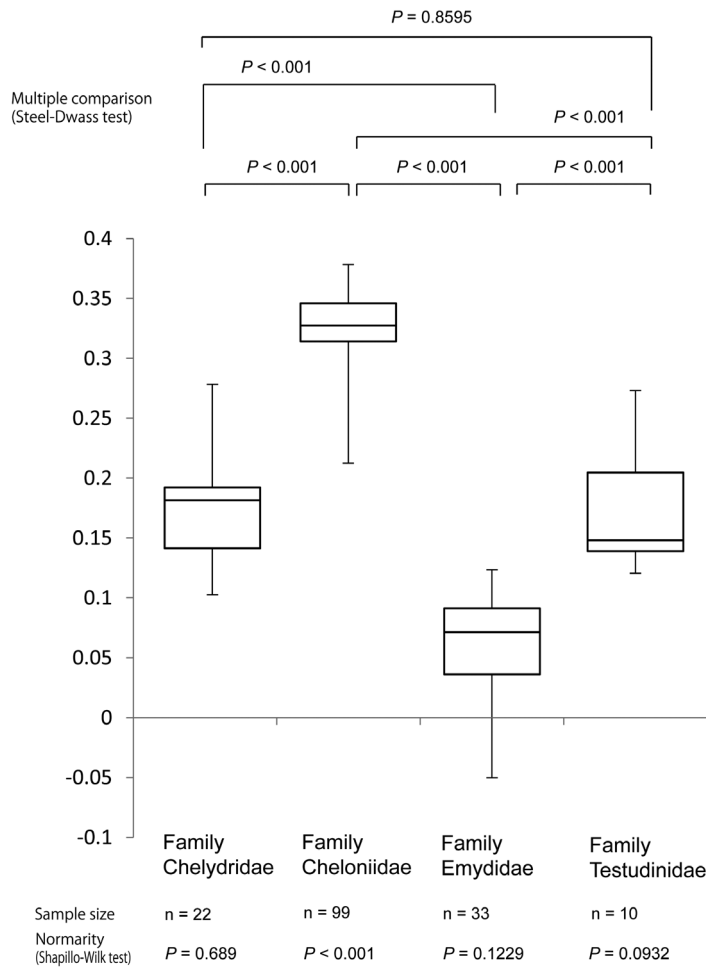


**Fig. 5.** Boxplot shows relative size of *foramen stapedio-temporalis* of family Chelydridae, Cheloniidae Emydidae, and Testudinidae. The normality of the distribution is tested by the Shapilko–Wilk test. Multiple comparison is conducted using the Steel–Dwass test.

scan of *Lo* reveals that lachrymal glands receives arterial blood not only from stapedia artery but also palatine artery (Fig. 3(2)). Therefore, rFST value itself is not enough to discuss the capacity of lachrymal glands. However, our findings indicate that cross section of FST is somehow correlated to the development of osmoregulation. The regression line we obtained from the scatter plot (Fig. 4) shows allometric growth of FST size in all examined specimens. It is considered that FST is prominent and developed structure in cranial circulation in earlier studies [3, 26, 34], but the size of FST basically grow as the body mass.

Our results also indicate a difference in rFST between the freshwater turtles family Chelydridae and Emydidae. Family Chelydridae samples of *Cs* and *Mt* were examined. Except for one sample of *Mt* (UMUT-21058), the rest are *Cs*. The examined samples of family Emydidae in this study were all *Ts*. Although the two have similar habitats and were sampled from a similar place, *Ts* had significantly smaller rFST than *Cs*. The rFST value of *Ts* was also significantly smaller than those for family Testudines.

*Ts* has a small rFST value than other turtles. According to earlier studies, the cranial arterial circulatory structures of family Chelydridae, family Emydidae, and family Testudinidae do not differ [27] and share similar pattern [25, 26]. However, rFST value of *Ts* is significantly smaller than other turtles and almost closed FST is observed on several specimens, *Ts* should not rely on stapedia artery in cranial circulation. It is necessary to study further anatomical structure, but pattern A [25, 26] may not include *Ts*.

Family Testudinidae samples examined is limited: *Centrochelys* (n=1), *Geochelone* (n=4), *Malacochers* (n=1), *Manouria* (n=1), *Stigmochelys* (n=1), and *Testudo* (n=2) (Table 1), although their known habitats are rather diverse. Our result suggests that there are

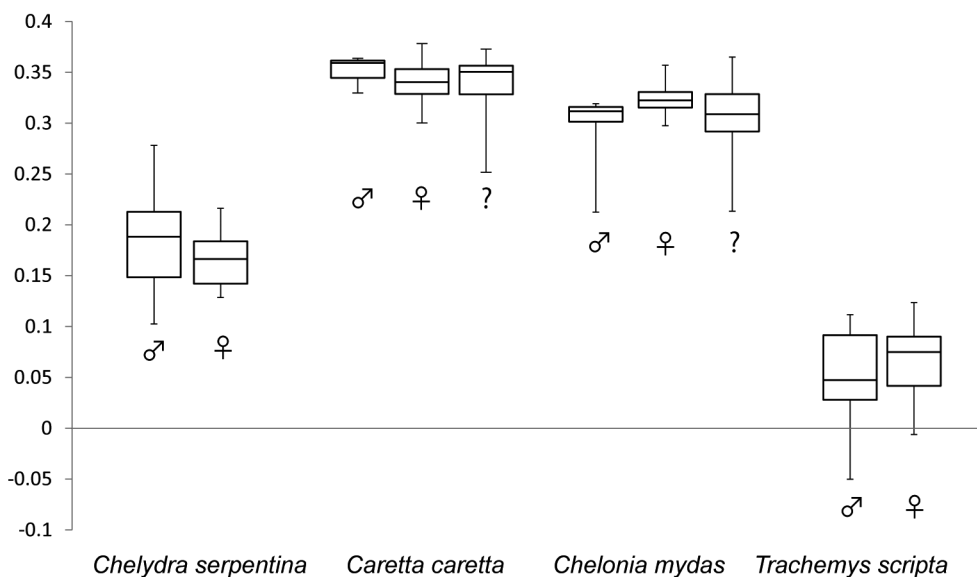


**Fig. 6.** Relative size of *foramen stapedio-temporalis* value of *Chelydra serpentina*, *Caretta caretta*, *Chelonia mydas*, and *Trachemys scripta*.

no significant differences ( $P=0.8595$ ) between family Chelydridae and Testudinidae (Fig. 5). The regression lines obtained from scatter plot (Fig. 4) also show two families share similar trend. Thus, terrestrial tortoises, may share common trends in rFST value with freshwater turtles. Considering the diverse habitats of family Testudinidae, ranging from forests to deserts, their physiological burden should also be diverse. Since the enlargement of the rFST value does not occur in family Testudinidae, their osmoregulation should be maintained in other ways. This matches to the earlier findings indicating that they can concentrate uric acid [4].

There was a significant difference in rFST for family Cheloniidae. *Cc* had a significantly larger rFST than *Cm*. Both *Cc* and *Cm* are completely marine-adapted animals and have fully functioning lacrimal glands for osmoregulation. The smaller rFST value of *Cm* should be sufficient for ocean dwelling life, so the larger rFST of *Cc* suggests a greater homeostatic burden. Diversity in the food habitat of sea turtles is well known. *Cc* are also omnivorous, eating crustaceans and shellfish throughout their lives [7, 40]. *Cm* are omnivorous until maturity and turn herbivorous when they mature and complete migration [8, 10]. The preference for feeding habits changes in response to the availability of food resources in their habitat [7]. Feeding habitat related morphological differences are recognized to exist between *Cc* and *Cm* [9, 48]. The contents of their blood plasma are also affected by the differences in their food habitats [46]. Phosphorous and sulfur in *Cm* and *Ei* blood plasma increase significantly in response to albuminous foods in captive environments. In addition, *Cc* maintains a lower potassium value than *Cm* and *Ei* both in and out of captive environments. This indicates that *Cc* has a better homeostatic function than other sea turtle species. Potassium is found in contents of excreted tear fluids of sea turtles [23], not phosphorous and sulfur. Lacrimal glands are involuntary organs and the ratio of potassium and sodium in tear fluids is fixed [37]. This fixed composition suggests that lacrimal glands are not responsible for excreting these excess electrolytes obtained from prey items. Further research is necessary to determine which organ is assigned for this homeostatic burden.

Another possible reason for the difference is the phylogenetic position of species. *Cc* belongs to tribe Caretini and *Cm* belongs to tribe Chelonini. To confirm the phylogenetic effects on rFST values, we should examine other family Cheloniidae members: *Natator depressus* of tribe Chelonini and *Ei*, *Lo*, and *Lepidochelys kempii* of tribe Caretini.

Besides the sea turtles completely adapted to marine life, several turtle species use blackish or marine water [2], including the Diamondback Terrapin *Malacley's terrapin* [12–14] and Common Snapping Turtle *Cs* [29, 30]. They are not ocean residents, but merely temporal visitors. In fossil records, several lineages also appear in oceanic sediments. These fossil records include evidence of adaptation to marine habitat. However, some of them may just be temporary visitors from marine environments, as is seen in extant species. Both extant and extinct turtles belong to the monophyletic order Testudines. For this phylogeny, one of the most parsimonious hypotheses is that the homeostatic function in turtles was developed through a common organ, the lacrimal glands in the orbital fossa.

The lacrimal gland, a necessary organ for electrolyte homeostasis is supplied by branches of stapedial artery in pattern A [25, 26] turtles. Turtles with other circulatory pattern are considered to be having different artery for supplying lacrimal glands. The major candidate route should be palatine artery, but not yet confirmed. Therefore, the development of FST and its relationship to lacrimal glands should be only effective in turtles with the circulatory pattern A.

One exception would be land tortoises (family Testudinidae) who can concentrate uric acid [4]. Nonetheless, the lacrimal gland's capability should be enlarged in response to the homeostatic burdens indicated in their evolutionary history. Suppose we hypothesize that the capability of lacrimal glands per cubic volume or per volume does not differ in order Testudines. In that case, it is possible to identify the homeostatic capability of both extant and extinct turtle species from their size of lacrimal glands. The current result shows that rFST value can be an index for marine adaptation in turtles. It can be used to analyze the adaptations of fossil marine turtles. Although body size may pose a difficulty, evolutionary trends can be seen in the group of similar skull proportions to the post cranium.

CONFLICT OF INTEREST. The authors have nothing to disclose.

ACKNOWLEDGMENTS. The research was financially supported by the Sasakawa Scientific Research Grant from The Japan Science Society (Masataka Yoshida, 2019), JSPS KAKENHI Grant Number JP 19H00534 and JP20H01381 from Japan Society for the Promotion of Science. Authors are very grateful to Drs Ryoko MATSUMOTO and Hajime TARU of Kanagawa Prefectural Museum of Natural History and Dr Shin-ichiro KAWADA and Ms Hiroko NAGAOKA of National Museum of Nature and Science, Japan for providing access to specimens. MY is especially grateful for Dr Takanobu Tsuihiji (National Museum of Nature and Science) for giving instruction of vessel injection, Mr Seiichiro TAKEDA and Mr Takashi TANIO (The University of Tokyo) for the assistance during specimen managements at UMUT, and Professor Ren HIRAYAMA (Waseda University) for introducing the field of turtle evolution. Authors are also very grateful to two anonymous peer reviewers for their helpful comments.

## REFERENCES

1. Abel, J. H. Jr. and Ellis, R. A. 1966. Histochemical and electron microscopic observations on the salt secreting lacrymal glands of marine turtles. *Am. J. Anat.* **118**: 337–357. [Medline] [CrossRef]
2. Agha, M., Ennen, J. R., Bower, D. S., Nowakowski, A. J., Sweat, S. C. and Todd, B. D. 2018. Salinity tolerances and use of saline environments by freshwater turtles: implications of sea level rise. *Biol. Rev. Camb. Philos. Soc.* **93**: 1634–1648. [Medline] [CrossRef]
3. Albrecht, P. W. 1976. The cranial arteries of turtles and their evolutionary significance. *J. Morphol.* **149**: 159–182. [Medline] [CrossRef]
4. Averill-Murray, R. C. 2002. Effects on survival of desert tortoises (*Gopherus agassizii*) urinating during handling. *Chelonian Conserv. Biol.* **4**: 430–435.
5. Baccari, G. C., Minucci, S. and Di Matteo, L. 1993. The orbital glands of the terrapin *Pseudemys scripta* in response to osmotic stress: a light and



- electron microscope study. *J. Anat.* **183**: 21–33. [[Medline](#)]
6. Chieffi Baccari, G., DiMatteo, L. and Minucci, S. 1992. The orbital glands of the chelonians *Pseudemys scripta* and *Testudo graeca*: comparative histological, histochemical and ultrastructural investigations. *J. Anat.* **180**: 1–13. [[Medline](#)]
  7. Bjorndal, K. A. 1997. Foraging ecology and nutrition of sea turtles. pp. 199–231. In: *The Biology of Sea Turtles* (Lutz, P. L. and Musick, J. A. eds.), CRC Press, Boca Raton.
  8. Bjorndal, K. A. 1980. Nutrition and grazing behavior of the green turtle *Chelonia mydas*. *Mar. Biol.* **56**: 147–154. [[CrossRef](#)]
  9. Brinkman, D. D. 2009. A sea turtle skull (Cheloniidae: Caretini) from the lower Miocene Nye Formation of Oregon, U.S.A. *Paludicola*. **7**: 39–46.
  10. Carrion-Cortez, J. A., Zárate, P. and Seminoff, J. A. 2010. Feeding ecology of the green sea turtle (*Chelonia mydas*) in the Galapagos Islands. *J. Mar. Biol. Assoc. U. K.* **90**: 1005–1013. [[CrossRef](#)]
  11. Chittick, B. and Harms, C. 2001. Intraocular pressure of juvenile loggerhead sea turtles (*Caretta caretta*) held in different positions. *Vet. Rec.* **149**: 587–589. [[Medline](#)] [[CrossRef](#)]
  12. Cowan, F. B. M. 1969. Gross and microscopic anatomy of the orbital glands of *Malaclemys* and other emydine turtles. *Can. J. Zool.* **47**: 723–729. [[CrossRef](#)]
  13. Cowan, F. B. M. 1990. Does the lachrymal salt gland of *Malaclemys terrapin* have a significant role in osmoregulation? *Can. J. Zool.* **68**: 1520–1524. [[CrossRef](#)]
  14. Cowan, F. B. M. 1981. Effects of salt loading on salt gland function in the euryhaline turtle, *Malaclemys terrapin*. *J. Comp. Physiol.* **145**: 101–108. [[CrossRef](#)]
  15. Cowan, F. B. M. 1971. The ultrastructure of the lachrymal ‘salt’ gland and the Harderian gland in the euryhaline *Malaclemys* and some closely related stenohaline emydines. *Can. J. Zool.* **49**: 691–697. [[Medline](#)] [[CrossRef](#)]
  16. Cowan, F. B. M. 1973. The homology of cranial glands in turtles: with special reference to the nomenclature of salt glands. *J. Morphol.* **141**: 157–169. [[Medline](#)] [[CrossRef](#)]
  17. Ellis, R. A. and Abel, J. H. Jr. 1964. Intercellular channels in the salt secreting glands of marine turtles. *Science* **144**: 1340–1342. [[Medline](#)] [[CrossRef](#)]
  18. Fänge, R., Schmidt-Nielsen, K. and Robinson, M. 1958. Control of secretion from the avian salt gland. *Am. J. Physiol.* **195**: 321–326. [[Medline](#)] [[CrossRef](#)]
  19. Fedorov, A., Beichel, R., Kalpathy-Cramer, J., Finet, J., Fillion-Robin, J. C., Pujol, S., Bauer, C., Jennings, D., Fenessy, F., Sonka, M., Buatti, J., Aylward, S., Miller, J. V., Pieper, S. and Kikinis, R. 2012. 3D Slicer as an image computing platform for the Quantitative Imaging Network. *Magn. Reson. Imaging* **30**: 1323–1341. [[Medline](#)] [[CrossRef](#)]
  20. Gaffney, E. S. 1984. Historical analysis of theories of chelonian relationship. *Syst. Zool.* **33**: 283. [[CrossRef](#)]
  21. Gaffney, E. S. 1979. Comparative cranial morphology of recent and fossil turtles. *Bull. Am. Mus. Nat. Hist.* **164**: 67–376.
  22. Hildebrand, M. and Goslow, G. 2001. *Analysis of Vertebrate Structure*, 5th ed., John Wiley & Sons, New York.
  23. Holmes, W. N. and McBean, R. L. 1964. Some aspects of electrolyte excretion in the green turtle, *Chelonia mydas mydas*. *J. Exp. Biol.* **41**: 81–90. [[Medline](#)] [[CrossRef](#)]
  24. Iverson, J. B. and Lewis, E. L. 2018. How to measure a turtle. *Herpetol. Rev.* **3**: 453–460.
  25. Jamniczky, H. A. 2008. Turtle carotid circulation: a character analysis case study. *Biol. J. Linn. Soc. Lond.* **93**: 239–256. [[CrossRef](#)]
  26. Jamniczky, H. A. and Russell, A. P. 2004. Cranial arterial foramen diameter in turtles: a quantitative assessment of size-independent phylogenetic signal. *Anim. Biol. Leiden Neth.* **54**: 417–436. [[CrossRef](#)]
  27. Jamniczky, H. A. and Russell, A. P. 2007. Reappraisal of patterns of nonmarine cryptodiran turtle carotid circulation: evidence from osteological correlates and soft tissues. *J. Morphol.* **268**: 571–587. [[Medline](#)] [[CrossRef](#)]
  28. Joyce, W. G. 2007. Phylogenetic relationships of mesozoic turtles. *Bull. Peabody Mus. Nat. Hist.* **48**: 3–102. [[CrossRef](#)]
  29. Kinneary, J. J. 1993. Salinity relations of *Chelydra serpentina* in a Long Island Estuary. *J. Herpetol.* **27**: 441. [[CrossRef](#)]
  30. Kinneary, J. J. 2021. Perspectives on salinity, immunity, and the common snapping turtle. *Chelonian Conserv. Biol.* **20**: 144–148. [[CrossRef](#)]
  31. Kooistra, T. A. and Evans, D. H. 1976. Sodium balance in the green turtle, *Chelonia mydas*, in seawater and freshwater. *J. Comp. Physiol.* **107**: 229–240. [[CrossRef](#)]
  32. Ku, D. N. 1997. Blood flow in arteries. *Annu. Rev. Fluid Mech.* **29**: 399–434. [[CrossRef](#)]
  33. Marn, N., Klanjscek, T., Stokes, L. and Jusup, M. 2015. Size scaling in Western North Atlantic loggerhead turtles permits extrapolation between regions, but not life stages. *PLoS One* **10**: e0143747. [[Medline](#)] [[CrossRef](#)]
  34. McDowell, S. B. 1961. On the major arterial canals in the ear-region of testudinoide turtles and the classification of the Testudinoidea. *Bull. Mus. Compar. Zool. Harvard.* **125**: 23–39.
  35. Natan, E., Fitak, R. R., Werber, Y. and Vortman, Y. 2020. Correction to ‘Symbiotic magnetic sensing: raising evidence and beyond’. *Philos. Trans. R. Soc. Lond. B Biol. Sci.* **375**: 20200348. [[Medline](#)] [[CrossRef](#)]
  36. Natan, E. and Vortman, Y. 2017. The symbiotic magnetic-sensing hypothesis: do *Magnetotactic Bacteria* underlie the magnetic sensing capability of animals? *Mov. Ecol.* **5**: 22. [[Medline](#)] [[CrossRef](#)]
  37. Nicolson, S. W. and Lutz, P. L. 1989. Salt gland function in the green sea turtle *Chelonia mydas*. *J. Exp. Biol.* **144**: 171–184. [[CrossRef](#)]
  38. Okamoto, K., Ouchi, Y., Ishihara, T. and Kamezaki, N. 2012. Straight carapace length calculation of the loggerhead and green sea turtles from some morphological characters. *Umigame Newsletter of Japan.* **91**: 8–12.
  39. Orós, J., Camacho, M., Calabuig, P. and Arencibia, A. 2011. Salt gland adenitis as only cause of stranding of loggerhead sea turtles *Caretta caretta*. *Dis. Aquat. Organ.* **95**: 163–166. [[Medline](#)] [[CrossRef](#)]
  40. Parker, D., Cooke, W. and Balazs, G. 2005. Diet of oceanic loggerhead sea turtles (*Caretta caretta*) in the Central North Pacific. *Fish Bull.* **103**: 142–152.
  41. Payne, A. P. 1994. The harderian gland: a tercentennial review. *J. Anat.* **185**: 1–49. [[Medline](#)]
  42. Reina, R. D. and Cooper, P. D. 2000. Control of salt gland activity in the hatchling green sea turtle, *Chelonia mydas*. *J. Comp. Physiol. B* **170**: 27–35. [[Medline](#)] [[CrossRef](#)]
  43. Reina, R. 2000. Salt gland blood flow in the hatchling green turtle, *Chelonia mydas*. *J. Comp. Physiol. B* **170**: 573–580. [[Medline](#)] [[CrossRef](#)]
  44. Rollet, Y., Evers, S. W. and Joyce, W. G. 2021. A review of the carotid artery and facial nerve canal systems in extant turtles. *PeerJ* **8**: e10475. [[Medline](#)] [[CrossRef](#)]
  45. Schmidt-Nielsen, K. and Fänge, R. 1958. Salt glands in marine reptiles. *Nature* **182**: 783–785. [[CrossRef](#)]
  46. Suzuki, K., Noda, J., Yanagisawa, M., Kawazu, I., Sera, K., Fukui, D., Asakawa, M. and Yokota, H. 2012. Particle-induced X-ray emission analysis of elements in plasma from wild and captive sea turtles (*Eretmochelys imbricata*, *Chelonia mydas*, and *Caretta caretta*) in Okinawa, Japan. *Biol. Trace Elem. Res.* **148**: 302–308. [[Medline](#)] [[CrossRef](#)]
  47. Wabnitz, C. and Pauly, D. 2008. Length–weight relationships and additional growth parameters for sea turtles. *Fish. Cent. Res. Rep.* **10**: 92–101.
  48. Wyneken, J. 2001. *The anatomy of sea turtles*. U.S. Department of Commerce NOAA Technical Memorandum. **470**: 1–172.
  49. Yoshida, M. and Endo, H. 2020. *Catalogue of the Collection of Turtle Specimens*, The University Museum, The University of Tokyo, Tokyo.